EUROPEAN ORGANIZATION FOR NUCLEAR RESEARCH

Proposal to the ISOLDE and Neutron Time-of-Flight Committee

Measuring the electron affinity of polonium

11th of January 2023

M.Nichols[1], M. Athanasakis-Kaklamanakis[2,3], Y. Balasmeh[3], A. Borschevsky[4], T. E. Cocolios[3], R. Crosa-Rossa[4], R. P. de Groote[3], C. Fajordo-Zambrano[3], K. T. Flanagan[5], R. F. Garcia Ruiz[6], D. Hanstorp[1], Á. Koszorús[3,7], L. Lalanne[2,3], D. Leimbach[1], Y.C. Liu[8], Y.S. Liu[8], K. M. Lynch[5], A. McGlone[5], G. Neyens[3], F. Pastrana[6], J. Reilly[5], S. Rothe[2], J. Trujillo[3], B. van den Borne[3], S. G. Wilkins[6], and X. F. Yang[8] for the CRIS Collaboration

[1] University of Gothenburg, SE-41296 Gothenburg, Sweden
[2] CERN, CH-1211 Geneva 23, Switzerland
[3] KU Leuven, B-3001 Leuven, Belgium
[4] University of Groningen, 9712 CP Groningen, The Netherlands
[5] The University of Manchester, Manchester M13 9PL, United Kingdom
[6] Massachusetts Institute of Technology, Cambridge, MA 02139, USA
[7] Belgian Nuclear Research Centre (SCK•CEN), Boeretang 200, 2400, Mol, Belgium
[8] Peking University, Beijing 100871, China

Spokesperson(s): Miranda Nichols (miranda.nichols@physics.gu.se)
Dag Hanstorp (dag.hanstorp@physics.gu.se)
Contact person: Louis Lalanne (louis.lalanne@kuleuven.be)

Abstract
We propose to measure the electron affinity (EA) of polonium by studying the onset of the photodetachment process $Po^- + hf \rightarrow Po + e^-$. This measurement follows the previously endorsed and completed INTC-I-225 letter of intent [1].

The main motivation to study negative ions is that the electron-electron correlation is more prevalent in negative ions than in neutral atoms or positive ions. Therefore, measurements of EAs can be used to test state of the art theoretical models that go beyond the independent particle model. The EA of most of the lighter elements has been measured, but experimental investigations on heavy ions, where relativistic effects become of great importance, are scarce. Furthermore, ^{210}Po is a toxic element of great importance for medical and environmental applications such as being a by-product of Gen IV fast reactors based on heavy liquid metal coolants. It is therefore of great interest to understand its chemical and physical properties.

Po$^-$ cannot be produced in the negative surface ion source used for the previous studies of negative ions at ISOLDE as its EA is smaller than the work function of the LaB$_6$ surface ionizer. We will instead produce Po$^-$ by double sequential electron capture in a charge exchange cell (CEC) available at CRIS, where we successfully have shown that negative ions can be produced (LOI-225). The photodetachment experiment will be conducted using the Gothenburg ANion Detector for Affinity measurements by Laser PHotodetachment (GANDALPH) which will be placed behind CRIS. There are no previous experimental investigations of the EA of Po, while calculations indicate it to be 1.469 eV.

Requested shifts: 15 shifts (+ 5 shifts of stable beam)

1

1   Introduction

The electron affinity (EA) is the amount of energy that is released when an electron binds to a neutral system to make it negative, i.e. the difference in energies of the ground states in the neutral atom and the negative ion. It is unusual for negative ions to have bound excited states due to the weak and shallow potential in which the valence electron is bound. This potential mainly arises from electron-electron correlation, which is a dominating effect in negative ions compared to neutral atoms or positive ions. Therefore, the EA is a value that can help us learn more about electron-electron correlation which in turn can be used to understand limitations of independent particle models [2].

Furthermore, by studying negative ions, we can learn about the chemical behaviour of elements and molecules such as reactivity and the stability of their chemical bonds because these properties are influenced by electron transfer [3]. Beyond their broad applications in fields such as medicine (e.g. radiopharmaceuticals [4]) and astrophysics [5], negative ions have applications at ISOLDE in future experiments at PUMA [6] which aims to produce antiprotonic ions by mixing antiprotons with negative ions. Precise EA measurements are then needed to benchmark theoretical models, which in the case of PUMA are needed to understand annihilation channels.

Determining EA values of increasingly heavy elements, especially those which are radioactive, aids in verifying the experimental technique as well as benchmarking theoretical models in atomic physics. In the work by Borschevsky *et al.* [7], the EAs of superheavy elements $_{115}$Mc, $_{116}$Lv and $_{117}$Tn were calculated using the relativistic coupled cluster approach [CCSD(T)] and compared with the homologous elements $_{83}$Bi, $_{84}$Po, and $_{85}$At. While the EA(Bi) [8] and EA(At) [9] have already been measured, determining the EA(Po) could further validate the computational approach and allow for higher accuracy predictions of the actinides and superheavy elements. As experiments grow increasingly difficult in these regions due to radioactivity, production yield, and laser requirements, accurate predictions are vital for successful experiments. The first radioactive negative ion photodetachment studies have been performed at ISOLDE, where ^{128}I$^-$ [10] and At$^-$ [9] were investigated.

Polonium (Po), element 84, is the first even-Z element in the periodic table for which all of the isotopes are radioactive, and most are short-lived. Polonium-210 ($t_{1/2}$=138.4 d) is a product of the ^{238}U decay chain. As an alpha emitter (E_α=5.29 MeV) with a high specific activity (166 TBq/g), ^{210}Po is highly toxic and potentially fatal when ingested [11]. Furthermore, the effect of ^{210}Po on the environment and human body is of high relevance in connection with mining of uranium. Therefore, further investigations are necessary so that efficient Po decorporation treatments and long-term management plans for abandoned uranium mines can be developed [12,13]. Po will also be produced in future Gen IV nuclear reactors cooled with heavy liquid metals, such as PbBi or PbLi eutectic. Finally, in the context of the MYRRHA Accelerator Driven System reactor development at the Belgian Nuclear Research Center SCK CEN, extensive investigations are currently ongoing to control the chemical behaviour of Po and its molecular forms as those might substantially impact the properties of the coolant [14].

The ionization potential (IP) of Po was measured with high precision at TRIUMF-ISAC [15] and ISOLDE [16]. The EA, on the other hand, remains experimentally unknown. Following the success of INTC-P-462 [17] for the EA determination of astatine (At) at ISOLDE [9], we now aim to measure the EA of Po. This is by itself very interesting and, in addition, a successful photodetachment study of Po$^-$ will open possibilities for photodetachment studies of other heavy elements with small electron affinities, such as francium and the actinides.

2. Experimental Method

2.1 Negative ion production

Beams of negative ions for the experiments determining the EAs of [128]I and [211]At have been produced using the ISOLDE MK4 negative surface ion source [18–20]. During these experiments it was found that Po[-] was not produced in sufficient quantities for photodetachment studies [17]. The reason for this is that Po has an EA which is significantly lower than the work function of LaB$_6$ (~2.6-2.9 eV) [19], which is the active surface in the ionizer. Therefore, another method of producing Po[-], and all other radioactive negative ions with low EA values, needs to be applied.

Producing negative ions by charge transfer from a beam of positive ions has been extensively studied in metal vapours [19,21–23]. Double sequential electron capture or double charge exchange involves the transfer of two electrons from a target vapor to the projectile element. This process depends on the projectile beam energy, the EA of the projectile, the IP of the charge exchange target vapor, and the vapor density [19,24]. The following reactions describe the double electron capture:

$$X^+ + Y \rightarrow X + Y^+ + \Delta E_1 \tag{1}$$

$$X + Y \rightarrow X^- + Y^+ + \Delta E_2 \tag{2}$$

Here X is the projectile beam, Y is the target vapor, and ΔE is the energy defect for the reaction. In the first electron capture (1), ΔE_1 is the equal to IP(X) – IP(Y), while in the second electron capture (2), ΔE_2 is equal to EA(X) – IP(Y). Negative ion yields are expected to be the highest when the energy defect, ΔE, for both reactions of the double electron capture process is as small as possible [19, 24].

We have already demonstrated that the method of producing negative ions of an element with a low EA in a charge exchange cell (CEC) works when we aimed to test negative ion production of [211]Po[-], [219]Fr[-], and [238]U[-] at CRIS in the INTC-I-225 letter of intent [1]. We successfully produced U[-] where the the negative ions were detected with a MagneToF detector. A projectile beam of U[+] at an energy of 40 keV was used together with a target alkali metal vapor of potassium (K). As mentioned in the previous paragraph, the vapor density in the CEC is a parameter that influences the production yield. In Fig. 1, negative ion production in arbitrary counts is shown as a function of the vapor temperature.

There is a third reaction to consider when producing a beam of negative ions by double charge exchange, namely

$$X^- + Y \rightarrow X + Y + e^-. \tag{3}$$

This reaction is important when the vapor density is sufficiently high for a third collision between projectile beam and target vapor in the CEC to occur, which destroys the negative ion. This can be seen in Fig. 1 when the count rate starts to decrease at ~136 °C. This curve was reversibly reproduced with both increasing and decreasing temperature. Unfortunately, we were unable to test the production of Po[-] (or Fr[-]) due to technical problems during the beamtime (mainly discharges in one of the electrodes in the CRIS beamline). Furthermore, the detection of Po[-] was obstructed due to positive ion contamination in the MagneToF detector which arose from being unable to efficiently separate positive from negative ions in the CRIS beamline. The necessary upgrades to solve this problem will be discussed in section 2.4. However, the rule of thumb for double charge exchange is that it scales with the EA. As uranium has an EA of 0.309 eV and the predicted EA of Po is 1.469 eV, we are convinced that we will be able to have a good yield of Po[-] production in the CEC.
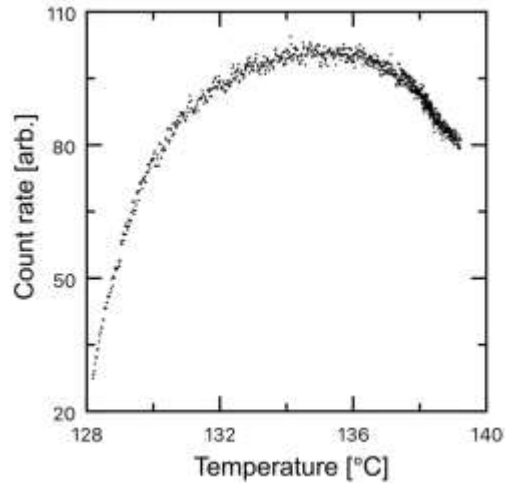
Figure 1: Temperature dependence of negative uranium-238 ion production in a charge exchange cell as measured with a MagneToF detector at CRIS. A projectile beam of $^{238}U^+$ ions with an energy of 40 keV collides with the alkali metal vapor target, potassium, to undergo a single electron capture reaction. The curve saturates at ~134°C. As pressure continues to increase, the cross section of a third collision increases in which the negative ions are subsequently destroyed. A similar temperature dependence was observed by Alton *et al.* [25] for production of Ca$^-$ on a lithium target.

2.2 Experimental technique

Laser photodetachment threshold (LPT) spectroscopy is a common technique used to measure EAs and has been successfully demonstrated at ISOLDE for radioactive $^{128}I^-$ [10] and At$^-$ [9]. In this method, the EA of an element is determined by the threshold photon energy that results in the onset of the photodetachment process, releasing a photoelectron from the negative ion and leaving a residual neutral atom. While scanning the photon energy, the residual neutral atoms are measured with a neutral particle detector (NPD) [26] where the yield can be directly related to the photodetachment cross section and remaining negative (or positive) ions are deflected from the beam. The neutralization rate scales to the Wigner law [27] which is governed by the angular momentum, l, of the detached electron. In the case of Po$^-$ that has a *p*-valence electron, the outgoing electron just above the threshold will be detached into an *s*-wave continuum ($l = 0$) due to electric dipole selection rules and centrifugal barrier suppression [1]. This gives rise to a sharp onset of photodetachment and can therefore be determined with high accuracy.

The experiment is performed in a collinear geometry, resulting in significantly improved statistics as compared with a crossed beams geometry due to the longer laser-ion interaction time resolution as compared to a cross beam geometry. Furthermore, the Doppler compression obtained by the accelerated beams improves the resolution [28]. y taking the geometrical mean of the measured EAs in the co- and counter-propagating directions of the laser-ion beam, the relativistic Doppler shift can be eliminated to all orders.

2.3 Theoretical preparation

Currently, the theoretical value of EA(Po) is reported to be 1.469 eV [4c+CCSD(T)+Breit+QED] [6]. An updated calculation of the EA(Po) will be carried out using the relativistic coupled cluster

approach. We will improve on this earlier work by using a higher quality basis set and by accounting for the effect of higher excitations, beyond perturbative triples (T). Furthermore, we will use an extensive computational study to set realistic uncertainties on our theoretical value, which should significantly facilitate the search of the EA signal. This approach was used, for example, to calculate the electron affinity of At prior to the measurements, and was shown to have excellent predictive power. The calculated result was just 2 meV below the experimental value, and this difference was well within the theoretical uncertainty.

The main motivation to improve the theoretical calculation is of course to be able to compare this with the experimental value and hence get an increased understanding of the fundamental interactions in the negative ions. However, a precise computational value is essential already in the planning of the experiment in order to guide the experiment to the correct wavelength region. The reported value of the EA of 1.469 eV suggests a scan over the threshold region in the wavelength range (833-849 nm). This can conveniently be produced using the fundamental output of a grating Ti:Sapphire laser available at CRIS. The spectral linewidth of the Ti:Sa laser (on the order of GHz) is adequate for the measurement. The beam path from the CRIS laser lab to the GANDALPH beamline behind CRIS, in co- and counter propagating directions, will be established and updated to comply with the laser safety standards of ISOLDE.

2.4 Experimental setup

We propose to perform the measurement at the CRIS beamline using its CEC for negative ion production with K vapour. A temperature readout of the CEC will be necessary for further investigations of double electron capture of heavy and radioactive elements. There are pre-existing resistive thermocouples which are used to read the relative temperature of the CEC. Upgrades will be made to this method so that actual pressure within the CEC can also be determined.
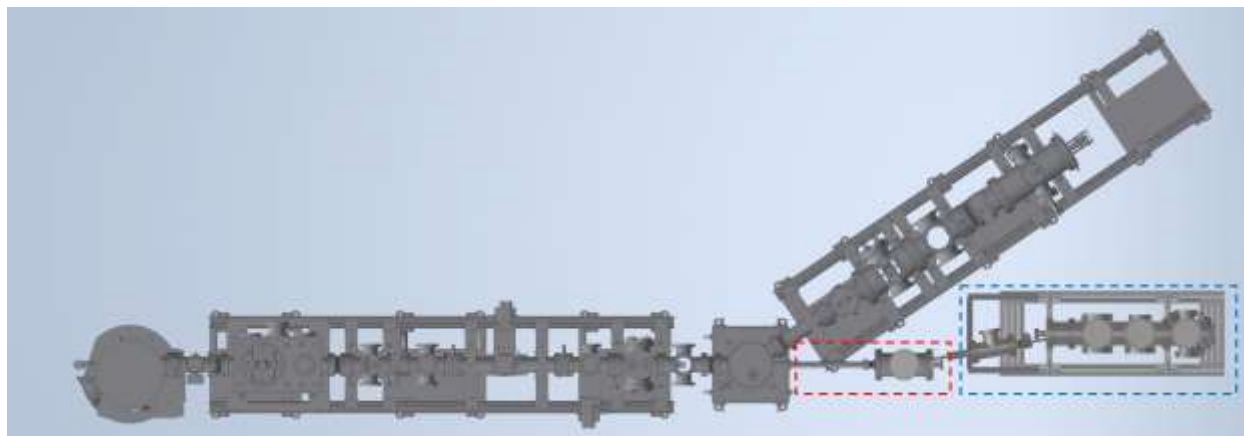

Figure 2: Outline of the footprint of the experimental system. The figure shows the planned updated version of the CRIS beamline (installation Q1 2023). The existing GANDALPH spectrometer, shown within the blue box, and a new chamber for focussing and deflection, shown within the red box will be added to this system. The latter is under construction at University of Gothenburg.

A new chamber will be added at the end of the CRIS beamline, shown within the red box in Figure 2, which will serve as a connecting point between CRIS and GANDALPH. The negative ions produced

5

in the CEC in CRIS will be bent into the GANDALPH spectrometer, shown within the blue box, by a 10-degree electrostatic bend located in the red box. The negative ions will then be guided through the differential pumping region which can achieve a vacuum of 10^{-9} mbar. In GANDALPH, the negative ions will be electrostatically bent by another 10 degrees. The laser and ion beams will then interact in the GANDALPH spectrometer which is defined by two collimators, as shown in Fig. 3. The co- and counter-propagating laser configurations will be achieved by two optical breadboards set up on both ends of GANDALPH. The laser will be transported by a combination of a multi-mode fiber and optical mirrors. The laser and data acquisition systems are already established parts of the CRIS experiment. The CRIS data tagger can be connected directly to the NPD to visualize real-time neutralization rates.
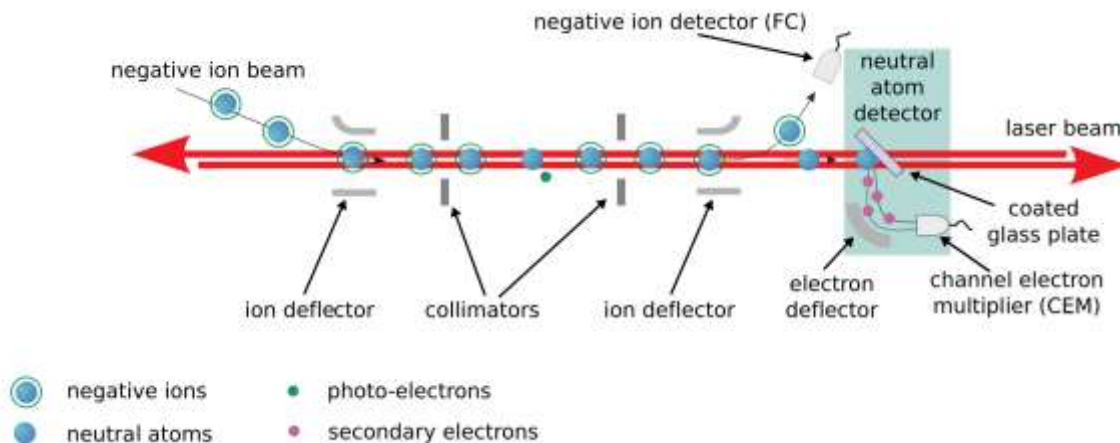
Figure 3: Collinear laser photodetachment threshold spectroscopy within the GANDALPH spectrometer. The frequency tuneable laser beam is overlapped with the negative ion beam. The laser is then tuned to an energy that is sufficient to photodetach an electron from the negative ion. The residual neutral atoms continue where they impinge on a graphene coated plate which generates secondary electrons which are then detected by a channel electron multiplier. These components make up the neutral particle detector (NPD). The measurement is performed in co- and counter-propagating directions to account for the Doppler shift.

3. Shift requirements

High production yields of Po isotopes have been demonstrated at ISOLDE by using actinide targets combined with laser ionization [29]. We aim to investigate an atomic property of Po, and we can therefore use any isotope that can be produced with sufficient yield. (We do not expect to observe an isotope shift in the EA since this would require a narrow bandwidth laser to be resolved). ^{202}Po was used in the experiments of LOI I-225 since it gives high yields and has relatively short-lived beam contaminants. However, the MagneToF detector contamination was too high rendering the detector unusable for nearly an entire shift.

Therefore, we are planning to utilise a different Po isotope, an ideal case in terms of beam purity being ^{211}Po (ground state $t_{1/2}$=516 ms, isomer $t_{1/2}$=25.2s) as it decays to stable ^{207}Pb. However, in-target production of ^{211}Po is expected to be three orders of magnitude lower than that of ^{202}Po (according to FLUKA calculations published in the Yield Database for UC$_x$ target), resulting in an expected yield of the order of 10^4 ions μC^{-1}, derived from a published yield of 1.7×10^7 ions μC^{-1} for ^{202}Po. This is supported by the I-225 experimental campaign, where ^{211}Po produced from the ISOLDE target in LIST mode was measured at the IDS experiment to be 14 000 counts/sec with a nearly pure beam. The transport efficiency from the end of ISCOOL to the end of the CRIS interaction region was about

5%. Hence, assuming the transport efficiency to the GANDALPH setup from the CRIS CEC as 1% [8] and the charge exchange efficiency with 30% [20], polonium beam yields should be at least 10^6 ions μC^{-1} to have sufficient ions reach the GANDLAPH interaction region, likely ruling out the use of ^{211}Po. However, as our experiment is isotope insensitive, any isotope produced in sufficient quantity, as is likely in the range of $^{193\text{-}205}$Po, such as i.e. ^{197}Po will suffice.

For the proposed experiment, we are requesting 4 offline shifts of ^{238}U which will serve as ion beam tuning and setup to the CRIS experiment. These shifts will also serve as the initial tests for negative ion production and detection. Following this, we request 15 shifts of online beamtime for the measurement of the EA of Po. We will need 3 shifts to reproduce the negative ion production curve in a CEC with Po. We then require 3 shifts to determine the initial photodetachment threshold scanning region. After this, we will use 9 shifts to perform the experimental measurement in co- and counter- propagating configurations.

In preparation for future proposals, we also request 1 shift for making an above threshold measurement for ^{238}U which will allow us to understand feasibility for eventually measuring the EA of U. This quantity has been measured using electron spectroscopy [30] and slow electron velocity map imaging [31]. By applying the technique of LPT we aim to improve the accuracy of this quantity. We also request 1 shift for producing and detecting Fr⁻, whose affinity also has not yet been determined experimentally. In total, we request 15 online shifts and 5 offline shifts for this experimental campaign.

1.1   Summary of requested shifts

We request a total of **15 online shifts** with 5 offline shifts beforehand for beam tuning, setup, and preliminary tests with U and Fr.

Description	Element	Number of shifts
Online		
Producing and detecting negative ions	Po	3
Determining threshold region	Po	3
Co- & counter-propagating scans	Po	9
Offline		
Beam tuning and setup	^{238}U	3
Above threshold measurement	^{238}U	1
Producing and detecting negative ions	Fr	1

References

[1]   M. Nichols, M. Athanasakis, M. L. Bissell, M. Block, A. Borschevsky, T. E. Cocolios, M. Duggan, E. Eliav, K. T. Flanagan, N. Galland, R. F. G. Ruiz, Y. Guo, D. Hanstorp, R. Heinke, D. Leimbach, Y. Liu, G. Neyens, A. Obertelli, H. A. Perrett, S. Raeder, J. Reilly, J. Warbinek, K. Wendt, F. Wienholtz, S. Wilkins, T. Chemistry, P. Division, O. Ridge, and D. Leimbach, *Letter of Intent to the ISOLDE and Neutron Time-of-Flight Committee Preparation of Negative Ion Beams for the Determination of the Electron Affinity of Polonium by Laser Photodetachment*, 1 (2021).

[2]   D. J. Pegg, *Structure and Dynamics of Negative Ions*, Reports Prog. Phys. **67**, 857 (2004).

[3]   J. C. Rienstra-Kiracofe, G. S. Tschumper, H. F. Schaefer III, S. Nandi, and G. Barney Ellison, *Atomic and Molecular Electron Affinities: Photoelectron Experiments and Theoretical Computations*, (2002).

[4]   D. Teze, D.-C. Sergentu, V. Kalichuk, J. Barbet, D. Deniaud, N. Galland, R. Maurice, and G. Montavon, *Targeted Radionuclide Therapy with Astatine-211: Oxidative Dehalogenation of Astatobenzoate Conjugates*, (n.d.).

[5]   T. J. Millar, C. Walsh, and T. A. Field, *Negative Ions in Space*, Chem. Rev. **117**, 1765 (2017).

[6]   T. Aumann, W. Bartmann, O. Boine-Frankenheim, A. Bouvard, A. Broche, F. Butin, D. Calvet, J. Carbonell, P. Chiggiato, H. De Gersem, R. De Oliveira, T. Dobers, F. Ehm, J. F. Somoza, J. Fischer, M. Fraser, E. Friedrich, A. Frotscher, M. Gomez-Ramos, J. L. Grenard, A. Hobl, G. Hupin, A. Husson, P. Indelicato, K. Johnston, C. Klink, Y. Kubota, R. Lazauskas, S. Malbrunot-Ettenauer, N. Marsic, W. F. O Müller, S. Naimi, N. Nakatsuka, R. Necca, D. Neidherr, G. Neyens, A. Obertelli, Y. Ono, S. Pasinelli, N. Paul, E. C. Pollacco, D. Rossi, H. Scheit, M. Schlaich, A. Schmidt, L. Schweikhard, R. Seki, S. Sels, E. Siesling, T. Uesaka, M. Vilén, M. Wada, F. Wienholtz, S. Wycech, and S. Zacarias, *PUMA, AntiProton Unstable Matter Annihilation: PUMA Collaboration*, Eur. Phys. J. A **58**, 1 (2022).

[7]   A. Borschevsky, L. F. Pašteka, V. Pershina, E. Eliav, and U. Kaldor, *Ionization Potentials and Electron Affinities of the Superheavy Elements 115-117 and Their Sixth-Row Homologues Bi, Po, and At*, Phys. Rev. A - At. Mol. Opt. Phys. **91**, 1 (2015).

[8]   R. C. Bilodeau and H. K. Haugen, *Electron Affinity of Bi Using Infrared Laser Photodetachment Threshold Spectroscopy*, Phys. Rev. A - At. Mol. Opt. Phys. **64**, 3 (2001).

[9]   D. Leimbach, J. Karls, Y. Guo, R. Ahmed, J. Ballof, L. Bengtsson, F. Boix Pamies, A. Borschevsky, K. Chrysalidis, E. Eliav, D. Fedorov, V. Fedosseev, O. Forstner, N. Galland, R. F. Garcia Ruiz, C. Granados, R. Heinke, K. Johnston, A. Koszorus, U. Köster, M. K. Kristiansson, Y. Liu, B. Marsh, P. Molkanov, L. F. Pašteka, J. P. Ramos, E. Renault, M. Reponen, A. Ringvall-Moberg, R. E. Rossel, D. Studer, A. Vernon, J. Warbinek, J. Welander, K. Wendt, S. Wilkins, D. Hanstorp, and S. Rothe, *The Electron Affinity of Astatine*, Nat. Commun. **11**, 1 (2020).

[10]   S. Rothe, J. Sundberg, J. Welander, K. Chrysalidis, T. D. Goodacre, V. Fedosseev, S. Fiotakis, O. Forstner, R. Heinke, K. Johnston, T. Kron, U. Köster, Y. Liu, B. Marsh, A. Ringvall-Moberg, R. E. Rossel, C. Seiffert, D. Studer, K. Wendt, and D. Hanstorp, *Laser Photodetachment of Radioactive 128I-*, J. Phys. G Nucl. Part. Phys. **44**, (2017).

[11]   B. Rego, *The Polonium Breif: A Hidden History of Cancer, Radiation, and the Tobacco Industry*, Isis **100**, 453 (2009).

[12]   F. Carvalho, S. Fernandes, S. Fesenko, E. Holm, B. Howard, P. Martin, M. Phaneuf, D. Porcelli, G. Pröhl, and J. Twining, The Environmental Behaviour of Polonium, 2017.

[13]   E. Ansoborlo, P. Berard, C. Den Auwer, R. Leggett, F. Menetrier, A. Younes, G. Montavon,

and P. Moisy, *Review of Chemical and Radiotoxicological Properties of Polonium for Internal Contamination Purposes*, Chem. Res. Toxicol. **25**, 1551 (2012).

[14] M. A. J. Mertens, A. Aerts, I. Infante, J. Neuhausen, and S. Cottenier, *Po-Containing Molecules in Fusion and Fission Reactors*, J. Phys. Chem. Lett. 2879 (2019).

[15] S. Raeder, H. Heggen, A. Teigelhöfer, and J. Lassen, *Determination of the First Ionization Energy of Polonium by Resonance Ionization Spectroscopy - Part I: Measurement of Even-Parity Rydberg States at TRIUMF-ISAC*, Spectrochim. Acta - Part B At. Spectrosc. **151**, 65 (2019).

[16] D. A. Fink, K. Blaum, V. N. Fedosseev, B. A. Marsh, R. E. Rossel, and S. Rothe, *Determination of the First Ionization Energy of Polonium by Resonance Ionization Spectroscopy – Part II: Measurement of Odd-Parity Rydberg States at CERN–ISOLDE*, Spectrochim. Acta - Part B At. Spectrosc. **151**, 72 (2019).

[17] S. Rothe, J. Champion, K. Chrysalidis, T. D. Goodacre, V. Fedosseev, N. Galland, D. Hanstorp, R. Heinke, T. Kron, B. Marsh, G. Montavon, E. Renault, R. Rossel, C. Seiffert, J. Sundberg, J. Welander, and K. Wendt, *Determination of the Electron Affinity of Astatine and Polonium by Laser Photodetachment*, INTC-P-462 (2016).

[18] M. Menna, R. Catherall, J. Lettry, E. Noah, and T. Stora, *R&D for the Development of Negative Ion Beams of Halogens*, Nucl. Instruments Methods Phys. Res. Sect. B Beam Interact. with Mater. Atoms **266**, 4391 (2008).

[19] Y. Liu, D. W. Stracener, and T. Stora, *Production of Negatively Charged Radioactive Ion Beams*, New J. Phys. **19**, (2017).

[20] U. Köster, *ISOLDE Target and Ion Source Chemistry*, Radiochim. Acta **89**, 749 (2001).

[21] J. Heinemeier and P. Hvelplund, *Production of 10-80 KeV Negative Heavy Ions by Charge Exchange in Na Vapour*, Nucl. Instruments Methods **148**, 425 (1978).

[22] J. Heinemeier and P. Hvelplund, *Production of 15-90 KeV Negative Heavy Ions by Charge Exchange with Mg Vapour*, Nucl. Instruments Methods **148**, 65 (1978).

[23] A. S. Schlachter, *Formation of Negative Ions by Charge Transfer: He- to Cl-**, AIP Conf. Proc. **300**, 300 (1984).

[24] G. D. Alton, *Negative Ion Formation Processes and Sources*, in *Negative-Ion Formation Processes and Sources. In: Hellborg, R. (Eds) Electrostatic Accelerators. Particle Acceleration and Detection.* (Springer, Berlin, Heidelberg, 2005), pp. 222–273.

[25] G. D. Alton, T. J. Kvale, R. N. Compton, D. J. Pegg, and J. S. Thompson, *The Production of Ca- through Sequential Charge Exchange with Li Vapor*, Nucl. Instruments Methods Phys. Res. A **244**, 142 (1986).

[26] J. Warbinek, D. Leimbach, D. Lu, K. Wendt, D. J. Pegg, A. Yurgens, D. Hanstorp, and J. Welander, *A Graphene-Based Neutral Particle Detector*, Appl. Phys. Lett. **114**, (2019).

[27] E. P. Wigner, *On the Behavior of Cross Sections Near Thresholds*, Phys. Rev. **73**, (1948).

[28] S. L. Kaufman, *High-Resolution Laser Spectroscopy in Fast Beams*, Opt. Commun. **17**, 309 (1976).

[29] T. E. Cocolios, B. A. Marsh, V. N. Fedosseev, S. Franchoo, G. Huber, M. Huyse, A. M. Ionan, K. Johnston, U. Köster, Y. Kudryavtsev, M. Seliverstov, E. Noah, T. Stora, and P. Van Duppen, *Resonant Laser Ionization of Polonium at Rilis-Isolde for the Study of Ground- and Isomer-State Properties*, Nucl. Instruments Methods Phys. Res. Sect. B Beam Interact. with Mater. Atoms **266**, 4403 (2008).

[30] S. M. Ciborowski, G. Liu, M. Blankenhorn, R. M. Harris, M. A. Marshall, Z. Zhu, K. H. Bowen, and K. A. Peterson, *The Electron Affinity of the Uranium Atom*, J. Chem. Phys. **154**, 224307 (2021).

[31] R. Tang, Y. Lu, H. Liu, and C. Ning, *Electron Affinity of Uranium and Bound States of Opposite Parity in Its Anion*, Phys. Rev. A **103**, 50801 (2021).

Appendix

DESCRIPTION OF THE PROPOSED EXPERIMENT

Please describe here below the main parts of your experimental set-up:

Part of the experiment	Design and manufacturing
CRIS experiment	☐ To be used without any modification X To be modified by extending it with GANDALPH
GANDALPH	X Collaboration responsible or equipment

HAZARDS GENERATED BY THE EXPERIMENT

Additional hazard from <u>flexible or transported</u> equipment to the CERN site:

Domain	Hazards/Hazardous Activities		Description
Mechanical Safety	Pressure	☐	[pressure] [bar], [volume][l]
	Vacuum	x	10^{-9} mbar
	Machine tools	☐	
	Mechanical energy (moving parts)	☐	
	Hot/Cold surfaces	☐	
Cryogenic Safety	Cryogenic fluid	☐	[fluid] [m³]
Electrical Safety	Electrical equipment and installations	☐	[voltage] [V], [current] [A]
	High Voltage equipment	x	5000 V
Chemical Safety	CMR (carcinogens, mutagens and toxic to reproduction)	☐	[fluid], [quantity]
	Toxic/Irritant	☐	[fluid], [quantity]
	Corrosive	☐	[fluid], [quantity]
	Oxidizing	☐	[fluid], [quantity]
	Flammable/Potentially explosive atmospheres	☐	[fluid], [quantity]
	Dangerous for the environment	☐	[fluid], [quantity]
Non-ionizing radiation Safety	Laser	x	Ti:Sa laser,class IV 833-849 nm
	UV light	☐	

	Magnetic field	☐	[magnetic field] [T]
Workplace	Excessive noise	☐	
	Working outside normal working hours	☐	
	Working at height (climbing platforms, etc.)	☐	
	Outdoor activities	☐	
Fire Safety	Ignition sources	☐	
	Combustible Materials	☐	
	Hot Work (e.g. welding, grinding)	☐	
Other hazards			